



HAL
open science

Mitochondrial dysfunction caused by novel ATAD3A mutations

Nathalie Dorison, Pauline Gaignard, Aurélien Bayot, Antoinette Gelot, Pierre Hadrien Becker, Salma Fourati, Elise Lebigot, Perrine Charles, Timothy Wai, Patrice Therond, et al.

► **To cite this version:**

Nathalie Dorison, Pauline Gaignard, Aurélien Bayot, Antoinette Gelot, Pierre Hadrien Becker, et al.. Mitochondrial dysfunction caused by novel ATAD3A mutations. *Molecular Genetics and Metabolism*, 2020, 10.1016/j.ymgme.2020.09.002 . hal-02964011

HAL Id: hal-02964011

<https://amu.hal.science/hal-02964011>

Submitted on 7 Jan 2021

HAL is a multi-disciplinary open access archive for the deposit and dissemination of scientific research documents, whether they are published or not. The documents may come from teaching and research institutions in France or abroad, or from public or private research centers.

L'archive ouverte pluridisciplinaire **HAL**, est destinée au dépôt et à la diffusion de documents scientifiques de niveau recherche, publiés ou non, émanant des établissements d'enseignement et de recherche français ou étrangers, des laboratoires publics ou privés.



Distributed under a Creative Commons Attribution - NonCommercial 4.0 International License

MITOCHONDRIAL DYSFUNCTION CAUSED BY NOVEL ATAD3A MUTATIONS

Nathalie DORISON^{1,2} Pauline GAINARD³, Aurélien BAYOT^{4,§}, Antoinette GELOT^{5,7}, Pierre Hadrien BECKER³, Salma FOURATI³, Elise LEBIGOT³, Perrine Charles⁶, Timothy WAI⁴, Patrice THEROND³, Abdelhamid SLAMA^{3*}.

1-Pediatric Neurosurgery Unit, Fondation Rothschild Hospital, Paris, France

2-Neuropediatric Unit, Hôpital Trousseau, APHP University, Paris, France

3-Biochemistry Department, Hôpital Bicêtre, APHP Université Paris-Saclay, Le Kremlin Bicêtre F-94275, France.

4-Mitochondrial Biology Group, Institut Pasteur, CNRS UMR 3691, Paris, France

5-Service d'anatomie pathologique, Hôpital Trousseau APHP, 26, avenue du Dr Arnold Netter 75571 Paris Cedex 12

6- Genetics department, neurogenetic reference center, Salpêtrière Hospital, 47 Boulevard de l'Hopital 75013, Paris France.

7-Aix-Marseille University, INSERM, INMED. Campus de Luminy, Marseille, France

§-Current address: Department of genetics, Hôpital Bichat, AP-HP. Nord – Université de Paris, 46 rue Henri Huchard, 75018 Paris, France

*Correspondence

Summary

Mitochondrial respiratory chain integrity depends on a number of proteins encoded by nuclear and mitochondrial genomes. Mutations of such factors can result in isolated or combined respiratory chain deficits, some of which can induce abnormal morphology of the mitochondrial network or accumulation of intermediary metabolites. Consequently, affected patients are clinically heterogeneous, presenting with central nervous system, muscular, or neurodegenerative disorders. *ATAD3A* is a nuclear-encoded ATPase protein of the AAA+ family and has been localized to the inner mitochondrial membrane. Recently reported mutations or large deletions in the *ATDA3A* gene in patients have been shown to induce altered mitochondrial structure and function and abnormal cholesterol metabolism in a recessive or dominant manner. Here, we report two siblings presenting axonal sensory-motor neuropathy associated with neonatal cataract. Genetic analyses identified two novel mutations in *ATAD3A*; a point mutation and an intronic 15 bp deletion affecting splicing and leading to exon skipping. Biochemical analysis in patient cells and tissues showed abnormal function of the mitochondrial respiratory chain in muscle and abnormal mitochondrial cristae structure. These new cases underline the large spectrum of biochemical and clinical presentations of *ATAD3A* deficiency and the different modes of inheritance, making it an atypical mitochondrial disorder

Introduction

ATAD3A is an inner mitochondrial membrane protein that interacts with MFN2, OPA1 and DNM1L, small GTPases that perform mitochondrial membrane fusion (MFN2, OPA1) and fission (DNM1L), suggesting that ATAD3A may be another mitochondrial protein with a role in mitochondrial dynamics[1]. In addition, ATAD3A has been implicated in mitochondrial DNA maintenance [2] and cholesterol metabolism [3]. In humans, ATAD3A is a nuclear-encoded ATPase protein of the AAA+ family and is a part of ATAD3 cluster genes constituted by three paralogs: ATAD3A, ATAD3B and ATAD3C which have an extensive sequence homology, but other species have only one ATAD3 locus [4]. The first mutations in *ATAD3A* leading to mitochondrial dysfunction were identified in eight patients from 7 families with distinct neurological syndromes associated to recurrent *de novo* mono-allelic or biallelic variations [5]. Five patients from the same family are heterozygous for the c.1582C>T, p.(Arg528Trp) mutation with a dominant-negative mechanism while the others patients have biallelic variants, two siblings with a homozygous c.158C>T p.(Thr53Ile) mutation and one patient with compound heterozygous deletions in the *ATAD3* gene cluster, *ATAD3A/ATAD3B* in one allele and *ATAD3A/ATAD3C* in the second allele. Later on, Cooper and coworkers [6] identified in 2017 another *ATAD3A de novo* mutation, c.1064G>A p.(Gly355Asp), in a woman presenting with spastic paraplegia and axonal neuropathy. Her son presented a dyskinetic cerebral palsy. Fibroblasts from these patients exhibited fragmented mitochondria and an upregulated autophagy. The authors demonstrated a dominant-negative effect of this mutation on the activity of the ATAD3A protein. The same year, another study [7] reported five subjects with a more severe phenotype, a fatal pontocerebellar hypoplasia associated with large biallelic deletions resulting from genomic rearrangement affecting the *ATAD3* gene cluster leading to altered cholesterol metabolism as then demonstrated in a mouse model of ATAD3 muscle deficiency [8]. Very recently, a large recurrent *de novo ATAD3* duplication was associated with fatal neonatal cardiomyopathy with corneal clouding and encephalopathy in 21 families [9,10]. To date, 48 affected patients have been documented

(summarized in Table 1) carrying recessive or dominant mutations and large deletions/duplications affecting the ATAD3 cluster genes [5–7,9,11–13].

Here we report the discovery of two new recessively inherited pathogenic variants in the *ATAD3A* gene, c.1609T>A, p.(Trp537Arg) and c.1614+2_1616+16del, p.(Arg503Profs*11) and related clinical and biochemical data. The patients are brother and sister from unrelated parents, presenting with axonal sensory-motor neuropathy associated with congenital cataracts and abnormal mitochondrial cristae morphology.

Material and methods

Patients: Two siblings from healthy non-consanguineous parents. Informed consent for diagnosis and research studies was obtained from their parents.

Biochemical studies

Respiratory chain activities were assessed in cultured skin fibroblasts and muscle biopsy as previously reported[14,15]. Cultured skin fibroblasts were grown in HAM F-10 medium (Eurobio, Les Ulis, France) supplemented with antibiotics (100 IU/mL penicillin and 100 µg/mL streptomycin), 50 mg/L uridine and 12% fetal bovine serum (FBS). Cells were cultured at 37°C in a humidified incubator with 5% CO₂.

Molecular Analysis

Genomic DNA was extracted from muscle or fibroblasts by standard methods. Mitochondrial DNA in muscle was analyzed qualitatively and quantitatively by long range PCR or qPCR respectively [16]. The high-throughput sequencing of total mtDNA and of a panel of 185 nuclear genes involved in the most common mitochondrial pathologies (gene list upon request) were performed by NGS on Illumina Miseq instrument. This panel was designed using the Agilent Sure select Design web Application. Preparation of genomic DNA for NGS analysis and bioinformatics workflow were performed as previously described [17]. Sanger

sequence was confirmed by PCR with specific primers to confirm detected mutations and allelic segregation from parents.

Total RNA was extracted from cultured skin fibroblasts, with or without emetine, using the EZ1 RNA Tissue mini kit (QIAGEN, Valencia, CA). Reverse-transcription was performed with the Omniscript Reverse Transcriptase kit (QIAGEN, Valencia, CA). The *ATAD3A* cDNA was amplified using two specific primers which frame exons 14, 15 and 16. After a 35-cycle amplification of the first strand cDNA corresponding to 50 ng of starting RNA, PCR products were subjected to 2% agarose gel electrophoresis. Sequencing reactions were carried out with the Big Dye Terminator cycle sequencing kit and analyzed with an ABI 3100 genetic analyzer (Applied Biosystems).

siRNA transfection

Reverse transfection of skin fibroblasts with siRNA was performed using Lipofectamine RNAiMAX reagent following manufacturer's instructions. Briefly, 160 μ L of PBS1X containing 0.8 μ L of 50 μ M siRNA and 1.6 μ L Lipofectamine RNAiMAX was incubated for 1h at room temperature. Then, 20 μ L per well of this transfection mixture was distributed in appropriate wells of a 96 well-plate before addition of 80 μ L per well of cell suspension at 50 000 cells/mL in complete DMEM medium (DMEM containing 4.5 g/L D-glucose, 2 mM glutamine as GlutaMAX, 1 mM sodium pyruvate, 10% FBS, 100 U/ml penicillin and 100 mg/ml streptomycin). Every single siRNA was transfected in triplicate in two independent control fibroblast cell lines. Non-Targeting siRNA Pool #2: Dharmacon D-001206-14-05; Human DNM1L1 siRNA SMART Pool: Dharmacon M-012092-01; YME1L siRNA: Dharmacon M-006103-01.

Immunofluorescence of mitochondria and microscopy

Skin fibroblasts were plated in a 96 well-plate at 6000 cells/well and grown in complete DMEM medium at 37°C in a humidified atmosphere containing 5% CO₂. After 24h, cells were washed once with warm PBS1X and immediately fixed with warm PFA 4% for 15 min,

followed by permeabilization in PBS1X-triton 0.1% for 5 min at room temperature and incubation overnight at 4°C in PBS1X-FBS 10%. Immunostaining of mitochondria was performed using an anti-TOM40 antibody (Proteintech: 18409-1-AP) diluted 1/1000 in PBS1X-FBS 5%, followed by incubation with an appropriate Alexa Fluor 488 fluorescent antibody. Immunofluorescence of transfected fibroblasts was performed after 72h of transfection in similar conditions as described above. Cells were imaged using an automated Operetta CLS confocal spinning disc microscope (PerkinElmer) in the confocal mode at the 20X magnification.

Quantification of mitochondrial morphology

Mitochondrial morphology was quantified using a machine learning approach developed with the Harmony 4.9 software (PerkinElmer) and based on a proprietary algorithm (PerkinElmer). Briefly, using texture parameters inherent to the software, the system was trained to discriminate 3 different classes of mitochondrial shape: Fragmented, Normal and Hyperfused. To this purpose, control fibroblast cells from two different healthy donors, exhibiting normal mitochondrial morphology, were transfected with siRNA directed against specific gene regulators of mitochondrial dynamics to induce either mitochondrial fragmentation (*YME1L1* siRNA), mitochondrial hyperfusion (*DNM1L* siRNA), or no effect (non-targeting NT siRNA). After 3 days of transfection, the 3 different classes of transfected cells were used for supervised machine learning, with at least 400 cells of each class originating from two independent control fibroblast cell lines from three independent transfected wells. After supervised training, cells were classified automatically into the 3 defined classes. To ensure the validity of the approach, all fibroblast cells (those used for machine learning and those of interest) were seeded, grown and immunostained in parallel in a single 96 well-plate.

Western-blotting

Total cell lysates were prepared on ice using RIPA buffer [150 mM NaCl, 1.0% IGEPAL® CA-630, 0.5% sodium deoxycholate, 0.1% SDS, 50 mM Tris, pH 8.0] (Sigma) supplemented with a protease inhibitor cocktail (Roche). Protein samples prepared in Laemmli buffer (BioRad) supplemented with 2-mercaptoethanol were separated by SDS-PAGE on a 4–20% Mini-PROTEAN® TGX™ Precast Protein Gel (BioRad). 50 µg of proteins were then electrotransferred onto a Hybond nitrocellulose membrane (GE Healthcare). Primary antibody binding was detected by incubation with a peroxidase-conjugated secondary antibody using Clarity™ Western ECL Substrate (BioRad). Details on primary antibodies are listed below: anti-ATAD3A polyclonal antibody is from Thermo Fisher Scientific (PA5-66727); anti-TUBULIN mouse monoclonal antibody is from Proteintech (HRP-66031); Total OXPHOS Human WB Antibody Cocktail, mouse monoclonal, is from abcam (ab110411).

Results:

Clinical and biochemical description

The first child of the siblings (II-1) was born to healthy non-consanguineous parents without perinatal problems and normal mensurations. He presented with bilateral congenital cataracts operated at 4 months, a strabismus operated at 6 months with residual nystagmus and ophthalmoplegia related to his visual defect (corrected visual acuity tends to 4 or 5/10 at adult age). Hypotonia with hyporeflexia was noticed since the first months of life; he learned to walk around the age of 3 years and axonal sensory-motor neuropathy was confirmed by electrophysiological studies. At 10 years of age, the child presented ataxic walking with foot deformities and used a wheelchair for extended mobility. By 26 years of age, he required the use of a cane for walking. He manifested pes equines and pes cavus with several foot surgeries in childhood. Arthrodesis was performed at 26 years of age to manage foot deformities.

He had a progressive growth delay (-2ds after 18 months) and at 19 years old weighed 41kg and stood 168 cm tall with a cranial perimeter of 56 cm (no endocrine investigation); at 26

years he weighed 60 kg, which is within the normal range. Clinical examination at this age showed cerebellar syndrome with ataxic gait, pes cavus, amyotrophy of the lower limbs with distal motor deficit, myoclonic tremor of upper limbs, generalized areflexia and distal lower limbs hypopallesthesia, complex severe ophthalmoplegia in all gaze positions with low visual acuity. Neither cardiac dysfunction nor hepatosplenomegaly were observed. He displayed normal cognitive and psychomotor development with normal MRI. Echocardiography was unremarkable with no indication of impaired cardiac function but cardiac MRI showed moderate enlargement of the left ventricle. The dentist reported enamel faults.

His sister (II-2) has a similar but more pronounced phenotype. She was born after an uneventful pregnancy with intrauterine growth retardation (height 47.5 cm; weight 3390 g). A bilateral congenital cataract was noted before 2 months of age and operated at the age of 10 months with residual strabismus, and low visual acuity. The motor delay with hypotonia and hyporeflexia was diagnosed within the first months of life; sitting was acquired at 12 months and autonomous walking at the age of 4 years. Electrophysiological studies were performed at 6 months of age and confirmed the sensory-motor neuropathy.

She had progressive amyotrophy and deformities of the feet, instability in walking with frequent falls and partial dependence on a wheelchair (independent walk 10 minutes / climb 2 floors). She underwent several orthopedic procedures for pes cavus. After 18 months she evolved with a growth delay of -3ds for weight and height and had a weak adipose panicle, repeated vomiting and tendency to anorexia. At 19 years old, her height was 145 cm and her weight was 34 kg. She reported normal menstrual cycles. The endocrine and nutritional assessments did not show any abnormalities (normal TSH, GH and IGF1 levels).

Clinical examination showed a severely ataxic gait, failure to sustain a stable standing position, pes cavus, recurvatum of the knees, distal motor deficits with amyotrophy, generalized areflexia, hypopallesthesia of the distal lower limbs, nystagmus and complete

ophthalmoplegia in all gaze positions. Corrected visual acuity was 2/10 left and right eyes with bilateral visual correction. Elocution and cognition were reported to be normal.

Brain MRIs were performed at 6 months, 8 and 13 years of age and remained normal although an optic neuropathy was suspected.

Cardiac ultrasound found a discreet enlargement of the posterior wall of the left ventricle at the 18 years of age but without clinical impact (annual monitoring). The dentist reported enamel faults (not reported in the unaffected brother).

Electrophysiological studies were performed at 6 months of age and confirmed the sensory-motor neuropathy. At 8 years old the values of motor nerve conduction study (NCS) parameters of the right common peroneal nerve were 1.6 millivolt for the distal amplitude, 1.1 for the proximal amplitude and 37.5 meter/second for the conduction velocity. The left posterior tibial nerve values were 1.5 millivolt for the distal amplitude, 1.1 for the proximal amplitude and 34.8 meter/second for the conduction velocity. The right median nerve values were 5.5 microvolt for the distal amplitude, 5.2 for the proximal amplitude and 51.8 meter/second for the conduction velocity. Distal sensitive latency were normal, for right median nerve values were 2 microvolt/ meter for sensitive distal amplitude, conduction velocity was incalculable.

Biochemical investigations of patient II-2 showed increased lactate concentrations in both blood (4.4, 5.7 mmol/l, reference values (RV)<1.8 mmol/l) and CSF (3.8 mmol/l, RV<1.8 mmol/l) with a high lactate/pyruvate ratio (20.7 and 19.8), thus leading us to further study energy metabolism with a particular focus on the mitochondrial respiratory chain activities in muscle and cultured fibroblasts of both patients. A decrease in complex I activity (46 nmol/min/mg of protein, RV: 60-123) for patient II-1 and a decrease in the activities of both complexes I (45 nmol/min/mg of protein, RV: 60-123) and III (386 nmol/min/mg of protein, RV: 1007-2465) for patient II-2 were identified in muscle but normal activities were measured in fibroblasts.

Molecular analysis

To identify the cause of the mitochondrial defect, we performed a mitochondrial DNA sequence analysis. We did not find any mutations, neither large deletions nor depletions of muscle mitochondrial DNA. High-throughput sequencing of a panel of 185 nuclear genes representing established mitochondrial genetic diseases and Sanger sequencing allowed us to identify, in both affected children, two novel compound heterozygous variants in the *ATAD3A* gene (NM_001170535): a point mutation c.1609T> A, p.(Trp537Arg) located in a highly conserved region of the exon 15, predicted to induce a deleterious amino acid change, and a 15 bps deletion c.1614+2_1616+16del, p.(Gln503Profs*11) resulting in exon 15 skipping as confirmed by cDNA analysis (Fig.1A, 1B). Parental analysis confirmed allelic segregation in agreement with an autosomal recessive inheritance. The c.1609T> A, p.(Trp537Arg) mutation was inherited from the mother while the c.1614+2_1616+16del, p.(Gln503Profs*11) was inherited from the father.

Western blot analysis:

Immunoblot analyses showed a profound reduction of ATAD3A protein in patient fibroblasts consistent with either protein instability or non-sense mediated decay of mRNA and loss of function. ATAD3B protein level was not affected (Fig. 2A). Analysis of subunits of mitochondrial respiratory chain complexes in patient fibroblasts also identified reduced steady state levels of both MTCO2 (complex IV subunit) and NDUFB8 (complex I subunit), whereas ATP5A (complex V subunit), UQCRC2 (complex III subunit) and SDHB (complex II subunit) were maintained at control levels (Fig. 2A).

Mitochondrial morphology:

Analysis of the mitochondrial network in patient fibroblasts by immunofluorescence and confocal microscopy did not show any evidence of abnormal mitochondrial morphology (Fig.

2B). Quantification of mitochondrial shape using a supervised machine learning approach showed no significant increase in fragmented mitochondria in fibroblasts from patients II-1 and II-2 as compared to controls (Fig. 2C). By contrast, electron microscopy analysis of skeletal muscles showed abnormal mitochondria (Fig. 3, A, B and C). The mitochondria were slightly increased in number with an abnormal morphology, their size was increased and their diameter was irregular due to the existence of constriction zones; in addition the cristae network was highly disturbed with elongated, non-parallel, branched crests, drawing alveoli in the cytoplasm.

Discussion:

Here we extend the number of patients with *ATAD3A* mutations and confirm the high clinical variability of the phenotype expressed in affected patients. The patients we described here are siblings from healthy unrelated parents and were identified to have novel biallelic variations: a novel c.1609T>A, p.(Trp537Arg) point mutation and an intronic 15 bp deletion c.1614+2_1616+16del, p.(Arg503Profs*11) resulting in exon 15 skipping and a premature stop codon. Western blot analyses showed that *ATAD3A* protein was undetectable in fibroblasts and the pedigree argues for a recessive mode of inheritance, excluding a dominant-negative effect of the truncated protein p.(Arg503Profs*11). Therefore, we can assume that the amino acid change p.(Trp537Arg) is an hypomorphic variant that cannot form stable *ATAD3A* oligomers.

These patients presented early ophthalmic abnormalities in the form of bilateral congenital cataracts, ophthalmoplegia and nystagmus, hypotonia and sensory-motor neuropathy, late-onset cardiac abnormalities without cognitive impairment. Up to now 48 patients from 38 families have been identified to carry pathogenic variants in *ATAD3A*; 29 patients have dominant variants, 9 patients with recessive single nucleotide variants and 10 patients have recessive deletions in the *ATAD3* gene cluster. Indeed, patients with *ATAD3A* disease, whether dominantly or recessively inherited, highlight the tremendous clinical heterogeneity and wide phenotypic spectrum caused by mutations in this gene (Table 1). As observed for

patients II-1 and II-2 described in this study, neuromuscular and ophthalmic signs are progressive and constantly present in patients with later onset. Our results suggest that congenital cataracts, which have previously been ascribed to the core phenotype of *ATAD3A* deficiency [5,13] may be an early sign of disease manifestation caused by recessive *ATAD3A* mutations. Congenital cataracts have previously been associated with pathogenic mutations in *MFN2*[18], *OPA1*[19] and other inborn errors of metabolism, but the underlying mechanism remains to be elucidated.

The recent description of recurrent *de novo* 68 kb duplication between exon 11 of *ATAD3A* and intron 7 of *ATAD3C* (with various breakpoints) has revealed two main clinical presentations associated with *ATAD3* cluster copy number variations: neonatal pontocerebellar hypoplasia caused by recessive homozygous deletions and hypertrophic or dilated cardiomyopathy caused by *de novo* dominant duplications. In the both cases, corneal clouding or cataract and encephalopathy were diagnosed and the death occurred in the first months of life.

Regarding point mutations, a genotype-phenotype correlation is more difficult to distinguish. Peralta *et al.* suggested that mutations affecting the C-terminal domain c.1217T>G, p.(Leu406Arg) could be more severe than those affecting the N-terminal domain (c.158C>T; p.(Thr53Ile), c.251T>C, p.(Thr84Met)), and it is consistent with the protein structure, since the C-terminal region with Walker A and Walker B domains constitutes the ATPase core of the protein whereas the N-terminal region contains two coiled-coil regions and two transmembrane domains TM1 and TM2, [20]. However, our description of two new patients with milder phenotypes and biallelic mutations in the C-terminal domain underlines that genotype-phenotype correlations are not straightforward.

Moreover, normal *ATAD3A* protein levels have been observed in fibroblasts from patients with a non-fatal phenotype (patients with dominant-negative variants p.(Arg528Trp) and p.(Gly355Asp), [5,6]) whereas *ATAD3A* was profoundly depleted in fibroblasts from patients that succumbed to their illness during the neonatal period (homozygous variant p.(Leu406Arg), [13]), leading to the notion that protein level of *ATAD3A* may be correlated to

the disease severity. Our data do not support this hypothesis, as we demonstrate that ATAD3A is undetectable in patients II-1 and II-2 fibroblasts even though they present a moderate phenotype.

The precise roles fulfilled by ATAD3 in mitochondria have yet to be fully clarified. Experimental studies show that ATAD3 is implicated in several functions within mitochondria: organization and structure of the inner mitochondrial membrane, mtDNA nucleoid organization, mitochondrial dynamics, and respiratory chain activity [1,2,5,8] and cholesterol import, which constitutes the first step of mitochondrial steroidogenesis [3,7]. How these pleiotropic effects are connected is not understood. These dysfunctions do not manifest concomitantly in all ATAD3-deficient patients, pointing to mutation-specific effects. Indeed, our study confirms that the mitochondrial structure is affected in ATAD3-deficiency patients: muscle biopsy of patients II-1 and II-2 showed giant mitochondria with severe cristae disorganization; abnormal cristae morphology with either small or swollen mitochondria have also been described in ATAD3-deficient fibroblasts [9,13]. mtDNA copy number was normal in muscle of patients II-1 and II-2, indicating that the severe alterations of the inner mitochondrial membrane do not necessarily lead to mtDNA depletion, as already underlined [13]. Our study did not examine nucleoid structure and thus we cannot exclude mtDNA aberrant organization as reported by Desai *et al* [7]. ATAD3 has been implicated in the regulation of mitochondrial dynamics, [2], although we did not observe significant alterations in mitochondrial morphology in patients II-1 and II-2 fibroblasts. In human fibroblasts, over-expression of p.Gly355Asp or the p.Lys358Arg variants, also located in the C-terminal domain, leads to increased mitochondrial fragmentation [6], although the effects on mitochondrial morphology caused by mutant ATAD3A proteins expressed at endogenous levels appears to be far more subtle. Our enzymatic studies showed that the respiratory chain function is sensitive to alterations of ATAD3: complex I deficiency (patient II-1) or combined deficiencies of complexes I and III (patient II-2) were identified in mitochondria isolated from muscle, as already described for some patients, but not all [5,10,13]. In contrast, we and others showed that ATAD3 defect did not induce a decrease of the

respiratory chain activity in fibroblasts, even though the quantity of some subunits was reduced which implies compensatory mechanism [5,6,8,10] and/or tissue-specific or cell type-specific thresholds for biochemical dysfunction. The recent study of Frazier *et al* highlighted well this tissue-specificity: complex I activity was more profoundly decreased in the heart than in skeletal muscle or in fibroblasts of ATAD3-deficient patients suffering from severe cardiomyopathy [10]. It stands to reason that the respiratory chain activity may be most severely compromised in the most clinically affected tissue.

In conclusion, our study helps to move our understanding of the physiological and pathophysiological relevance of ATAD3A forward. Identifying novel *ATAD3A* pathogenic variant will help to establish future genotype-phenotype correlations and delineate pathways of *ATAD3A*-related disorders.

SNV Allele 1 / allele 2	Inheritance Protein domain	Outcome	Symptoms	Sources
c.1217T>G, p.(Leu406Arg) / c.1217T>G, p.(Leu406Arg) (4p, 1F)	Recessive C-terminal	Death in NN period	Axial hypotonia, encephalopathy, cerebellar hypoplasia, congenital cataract, hypertrophic cardiomyopathy, hepatomegaly	[11]
c.490C>T, p.(Gln164*)/c.230T>G, p.(Leu77Arg) (2p, 1F)	Recessive Stop/N-terminal	Death in NN period	Calcification in basal ganglia, delayed gyration and white matter myelination, pontocerebellar hypoplasia, developmental delay, ataxia, cerebellar atrophy	[10]
c.158C>T, p.(Thr53Ile) / c.158C>T, p.(Thr53Ile) (2p, 1F)	Recessive N-terminal	Alive at 23 and 26 yrs	Developmental delay, seizure, congenital cataract, hypotonia, ataxia, speech delay, optic neuropathy, cerebellar atrophy	[5]
c.251T>C, p.(Thr84Met) / c.251T>C, p.(Thr84Met) (1p, 1F)	Recessive N-terminal	Alive at 4.5 yrs	Developmental delay, ocular motor apraxia, mild cerebellum atrophy. No cardiomyopathy, no optic atrophy	[9]
c.1609T>A, p.(Trp537Arg) / c.1614+2_1616+16del(p.Arg503Profs*11) (2P, 1F)	Recessive C-terminal	Alive at 19 and 26 yrs	Neonatal cataract, axonal sensorimotor neuropathy	This study
c.1582C>T, p.(Arg528Trp) / - (5p, 5F)	Dominant C-terminal	Alive at 2 to 6 yrs	Developmental delay (5/5), hypotonia (5/5), optic atrophy (3/5), axonal neuropathy, hypertrophic cardiomyopathy (2/5)	[5]
c.1064G>A, p.(Gly355Asp) / - (2p, 1F)	Dominant C-terminal	Alive 35 and 3.5 yrs	Spastic paraplegia, axonal neuropathy and photophobia. No hypertrophic cardiomyopathy, no optic atrophy	[6]
Deletions				
~38 kb del <i>ATAD3B-ATAD3A</i> / ~68 kb del <i>ATAD3C-ATAD3A</i> (1p, 1F)	Recessive	Death in NN period	Seizures, hypotonia, spasticity, corneal clouding, respiratory failure	[5]
38054 bp del <i>ATAD3B-ATAD3A</i> / 38054 bp del <i>ATAD3B-ATAD3A</i> (2p, 1F)	Recessive	Death in NN period	Pontocerebellar hypoplasia	[7]
38667 bp del <i>ATAD3B-ATAD3A</i> / 38667 bp del <i>ATAD3B-ATAD3A</i> (2p, 2F)	Recessive	Death in NN period	Pontocerebellar hypoplasia	[7]
38667 bp del <i>ATAD3B-ATAD3A</i> / 38054 bp del <i>ATAD3B-ATAD3A</i> (1p, 1F)	Recessive	Death at 7 months	Pontocerebellar hypoplasia	[7]
del <i>ATAD3A-ATAD3B</i> / del <i>ATAD3A-ATAD3B</i> (4p, 3F)	Recessive	Death in NN period	Pontocerebellar hypoplasia, delayed gyration	[10]
Duplications				
68 kb dup <i>ATAD3A-ATAD3B-ATAD3C</i> / - (22p, 21F)	Dominant	Death in NN period	Hypertrophic or dilated cardiomyopathy, corneal clouding or cataracts, hypotonia, encephalopathy, white matter change	[10,12]

Table 1: ATAD3A-reported cases. F: family, NN: Neonatal period, p: patient, SNV: Single Nucleotide variants.

Figures

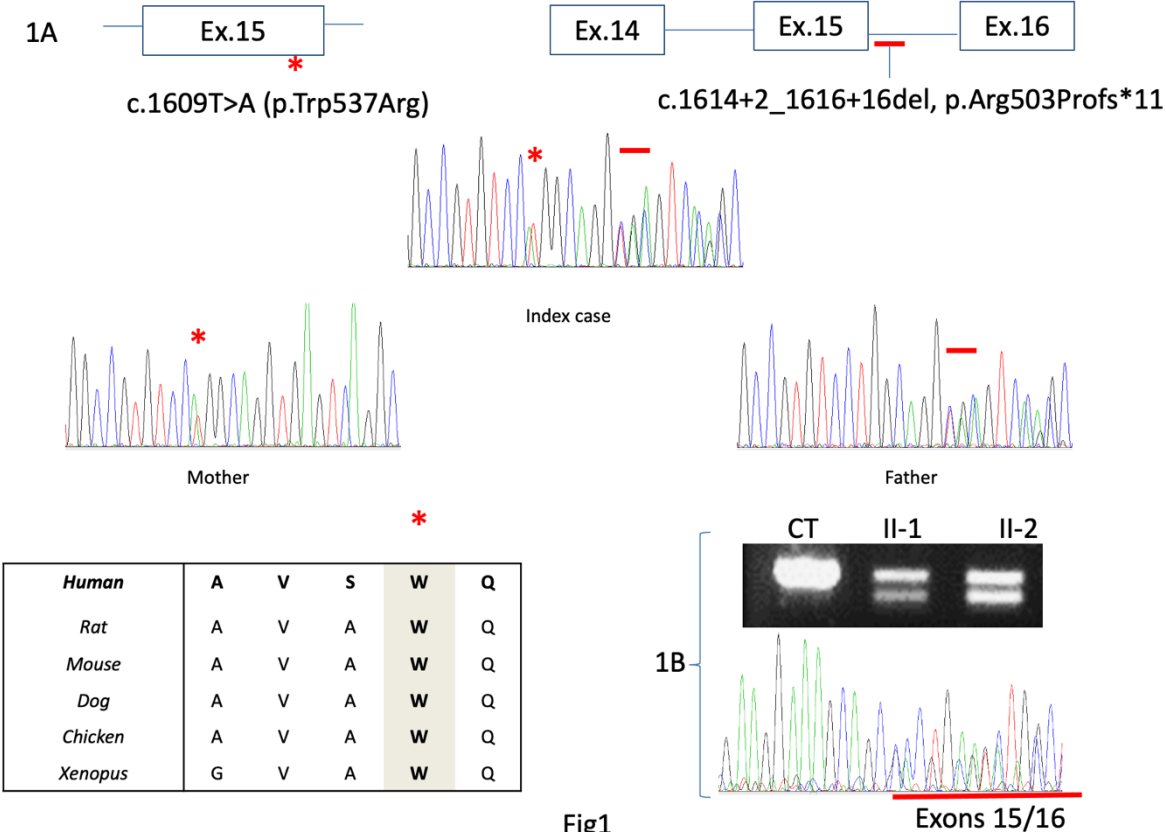


Fig. 1: Sanger sequencing validation of *ATAD3A* mutations situated in exon 15 from patient II-1 and her parents and multiple sequence alignment from NCBA orthologues sequence (1A). cDNA specific amplification of exon 14-15 and 16 by PCR and Sanger sequencing(1B)

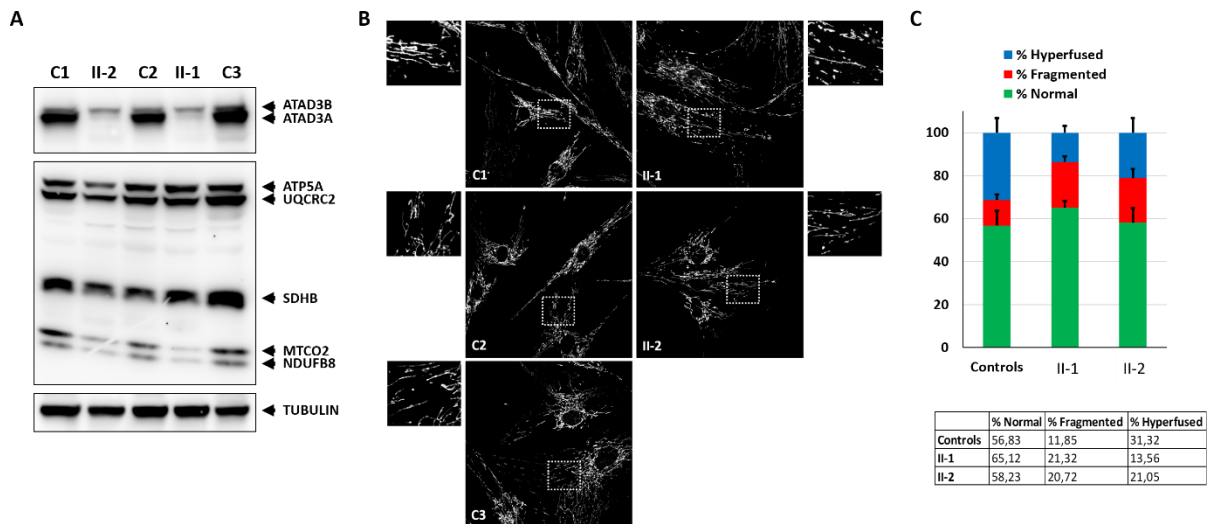


Fig. 2: Analysis of patient fibroblasts (II-1 and II-2) as compared to 3 independent controls (C1, C2, C3). **A.** Western-blot analysis of proteins (50 μ g per lane). TUBULIN is used as loading control. **B.** TOM40 immunofluorescence showing mitochondrial network. Enlarged zooms are shown in the insets. **C.** Quantification of mitochondrial morphology

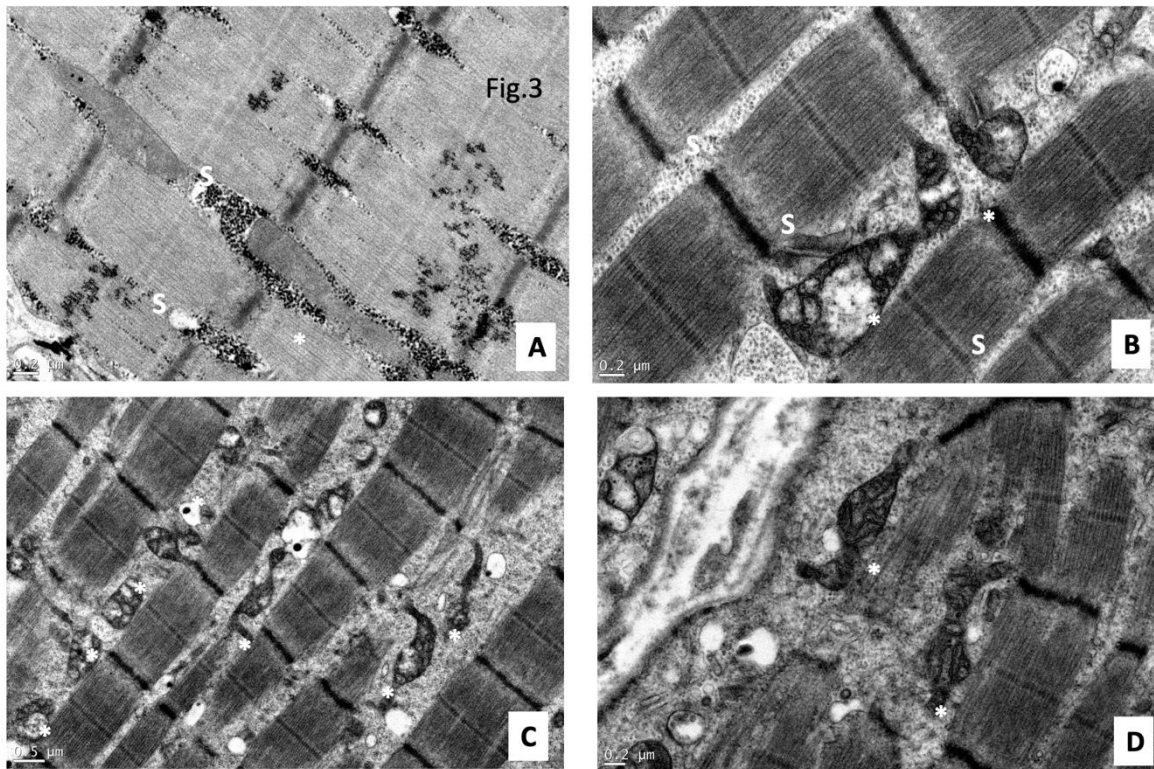


Fig 3

Fig. 3: Ultrastructure of the muscle

A : Control : 7 years-old- child ; **B , C,D** : Patient: 10 months : A,B,D : scale bar : 0,2 micrometers ; **C** : scale bar : 05 micrometers

In control patient, mitochondria (*) displayed constant diameters and parallel cristae in the affected patient mitochondria displayed abnormal size (giant) , shape (focal narrowings) and structure (cristae disorganization).

References

- [1] H.Y. Fang, C.L. Chang, S.H. Hsu, C.Y. Huang, S.F. Chiang, S.H. Chiou, C.H. Huang, Y.T. Hsiao, T.Y. Lin, I.P. Chiang, W.H. Hsu, S. Sugano, C.Y. Chen, C.Y. Lin, W.J. Ko, K.C. Chow, ATPase family AAA domain-containing 3A is a novel anti-apoptotic factor in lung adenocarcinoma cells, *J. Cell Sci.* 123 (2010) 1171–1180.
<https://doi.org/10.1242/jcs.062034>.
- [2] B. Gilquin, E. Taillebourg, N. Cherradi, A. Hubstenberger, O. Gay, N. Merle, N. Assard, M.-O. Fauvarque, S. Tomohiro, O. Kuge, J. Baudier, The AAA+ ATPase ATAD3A Controls Mitochondrial Dynamics at the Interface of the Inner and Outer Membranes, *Mol. Cell. Biol.* 30 (2010) 1984–1996. <https://doi.org/10.1128/mcb.00007-10>.
- [3] M.B. Rone, A.S. Midzak, L. Issop, G. Rammouz, S. Jagannathan, J. Fan, X. Ye, J. Blonder, T. Veenstra, V. Papadopoulos, Identification of a dynamic mitochondrial protein complex driving cholesterol import, trafficking, and metabolism to steroid hormones, *Mol. Endocrinol.* 26 (2012) 1868–1882. <https://doi.org/10.1210/me.2012-1159>.
- [4] S. Li, D. Rousseau, ATAD3, a vital membrane bound mitochondrial ATPase involved in tumor progression, *J. Bioenerg. Biomembr.* 44 (2012) 189–197.
<https://doi.org/10.1007/s10863-012-9424-5>.
- [5] T. Harel, W.H. Yoon, C. Garone, S. Gu, Z. Coban-Akdemir, M.K. Eldomery, J.E. Posey, S.N. Jhangiani, J.A. Rosenfeld, M.T. Cho, S. Fox, M. Withers, S.M. Brooks, T. Chiang, L. Duraine, S. Erdin, B. Yuan, Y. Shao, E. Moussallem, C. Lamperti, M.A. Donati, J.D. Smith, H.M. McLaughlin, C.M. Eng, M. Walkiewicz, F. Xia, T. Pippucci, P. Magini, M. Seri, M. Zeviani, M. Hirano, J. V. Hunter, M. Srour, S. Zanigni, R.A. Lewis, D.M. Muzny, T.E. Lotze, E. Boerwinkle, R.A. Gibbs, S.E. Hickey, B.H. Graham, Y.

- Yang, D. Buhas, D.M. Martin, L. Potocki, C. Graziano, H.J. Bellen, J.R. Lupski, Recurrent De Novo and Biallelic Variation of ATAD3A, Encoding a Mitochondrial Membrane Protein, Results in Distinct Neurological Syndromes, *Am. J. Hum. Genet.* 99 (2016) 831–845. <https://doi.org/10.1016/j.ajhg.2016.08.007>.
- [6] H.M. Cooper, Y. Yang, E. Ylikallio, R. Khairullin, R. Woldegebriel, K.L. Lin, L. Euro, E. Palin, A. Wolf, R. Trokovic, P. Isohanni, S. Kaakkola, M. Auranen, T. Lonqvist, S. Wanrooij, H. Tynismaa, ATPase-deficient mitochondrial inner membrane protein ATAD3a disturbs mitochondrial dynamics in dominant hereditary spastic paraplegia, *Hum. Mol. Genet.* 26 (2017) 1432–1443. <https://doi.org/10.1093/hmg/ddx042>.
- [7] R. Desai, A.E. Frazier, R. Durigon, H. Patel, A.W. Jones, I.D. Rosa, N.J. Lake, A.G. Compton, H.S. Mountford, E.J. Tucker, A.L.R. Mitchell, D. Jackson, A. Sesay, M. Di Re, L.P. Van Den Heuvel, D. Burke, D. Francis, S. Lunke, G. McGillivray, S. Mandelstam, F. Mochel, B. Keren, C. Jardel, A.M. Turner, P.I. Andrews, J. Smeitink, J.N. Spelbrink, S.J. Heales, M. Kohda, A. Ohtake, K. Murayama, Y. Okazaki, A. Lombès, I.J. Holt, D.R. Thorburn, A. Spinazzola, ATAD3 gene cluster deletions cause cerebellar dysfunction associated with altered mitochondrial DNA and cholesterol metabolism, *Brain.* 140 (2017) 1595–1610. <https://doi.org/10.1093/brain/awx094>.
- [8] S. Peralta, S. Goffart, S.L. Williams, F. Diaz, S. Garcia, N. Nissanka, E. Area-Gomez, J. Pohjoismäki, C.T. Moraes, ATAD3 controls mitochondrial cristae structure in mouse muscle, influencing mtDNA replication and cholesterol levels, *J. Cell Sci.* 131 (2018). <https://doi.org/10.1242/jcs.217075>.
- [9] A.C. Gunning, K. Strucinska, M. Muñoz Oreja, A. Parrish, R. Caswell, K.L. Stals, R. Durigon, K. Durlacher-Betzer, M.H. Cunningham, C.M. Grochowski, J. Baptista, C. Tysoe, E. Baple, N. Lahiri, T. Homfray, I. Scurr, C. Armstrong, J. Dean, U. Fernandez Pelayo, A.W.E. Jones, R.W. Taylor, V.K. Misra, W.H. Yoon, C.F. Wright, J.R. Lupski, A. Spinazzola, T. Harel, I.J. Holt, S. Ellard, Recurrent De Novo NAHR Reciprocal

- Duplications in the ATAD3 Gene Cluster Cause a Neurogenetic Trait with Perturbed Cholesterol and Mitochondrial Metabolism, *Am. J. Hum. Genet.* 106 (2020) 272–279. <https://doi.org/10.1016/j.ajhg.2020.01.007>.
- [10] A.E. Frazier, G. Alison, C. Simons, A.E. Frazier, A.G. Compton, Y. Kishita, D.H. Hock, A.E. Welch, S.S.C. Amarasekera, R. Rius, L.E. Formosa, J.S. Jabbari, A. Lucattini, K.R. Nitta, A. Ohtake, K. Murayama, Clinical and Translational Article Fatal Perinatal Mitochondrial Cardiac Failure Caused by Recurrent De Novo Duplications in the ATAD3 Locus Fatal Perinatal Mitochondrial Cardiac Failure Caused by Recurrent De Novo Duplications in the ATAD3 Locus, (2020) 1–25. <https://doi.org/10.1016/j.medj.2020.06.004>.
- [11] A. Al Madhoun, F. Alnaser, M. Melhem, R. Nizam, T. Al-Dabbous, F. Al-Mulla, Ketogenic diet attenuates cerebellar atrophy progression in a subject with a biallelic variant at the ATAD3A locus [response to letter], *Appl. Clin. Genet.* 12 (2019) 163–165. <https://doi.org/10.2147/TACG.S224520>.
- [12] C.M.P.C.D. Peeters-Scholte, P.N. Adama Van Scheltema, F.J.C.M. Klumper, S.M.P. Everwijn, M. Koopmans, M.J.V. Hoffer, T.T. Koopmann, C.A.L. Ruivenkamp, S.J. Steggerda, M.S. Van Der Knaap, G.W.E. Santen, Genotype-phenotype correlation in ATAD3A deletions: Not just of scientific relevance, *Brain.* 140 (2017) e66. <https://doi.org/10.1093/brain/awx239>.
- [13] S. Peralta, A. González-Quintana, M. Ybarra, A. Delmiro, R. Pérez-Pérez, J. Docampo, J. Arenas, A. Blázquez, C. Ugalde, M.A. Martín, Novel ATAD3A recessive mutation associated to fatal cerebellar hypoplasia with multiorgan involvement and mitochondrial structural abnormalities, *Mol. Genet. Metab.* 128 (2019) 452–462. <https://doi.org/10.1016/j.ymgme.2019.10.012>.
- [14] P. Rustin, D. Chretien, T. Bourgeron, B. Gérard, A. Rötig, J.M. Saudubray, A. Munnich, Biochemical and molecular investigations in respiratory chain deficiencies,

- Clin. Chim. Acta. 228 (1994) 35–51. [https://doi.org/10.1016/0009-8981\(94\)90055-8](https://doi.org/10.1016/0009-8981(94)90055-8).
- [15] D. Chretien, P. Rustin, T. Bourgeron, A. Rötig, J.M. Saudubray, A. Munnich, Reference charts for respiratory chain activities in human tissues, Clin. Chim. Acta. 228 (1994) 53–70. [https://doi.org/10.1016/0009-8981\(94\)90056-6](https://doi.org/10.1016/0009-8981(94)90056-6).
- [16] B. Chabi, B. Mousson De Camaret, H. Duborjal, J.P. Issartel, G. Stepien, Quantification of mitochondrial DNA deletion, depletion, and overreplication: Application to diagnosis, Clin. Chem. 49 (2003) 1309–1317. <https://doi.org/10.1373/49.8.1309>.
- [17] N. Bouali, B. Francou, J. Bouligand, D. Imanci, S. Dimassi, L. Tosca, M. Zaouali, S. Mougou, J. Young, A. Saad, A. Guiochon-Mantel, New MCM8 mutation associated with premature ovarian insufficiency and chromosomal instability in a highly consanguineous Tunisian family, Fertil. Steril. 108 (2017) 694–702. <https://doi.org/10.1016/j.fertnstert.2017.07.015>.
- [18] J. Zhao, X. Wu, D. Wu, Y. Yu, Y. Yu, Y. Wang, Q. Fu, J. Zhang, K. Yao, Embryonic Surface Ectoderm-specific Mitofusin 2 Conditional Knockout Induces Congenital Cataracts in Mice, Sci. Rep. 8 (2018) 1–11. <https://doi.org/10.1038/s41598-018-19849-2>.
- [19] J. Lee, S.C. Jung, Y. Bin Hong, J.H. Yoo, H. Koo, J.H. Lee, H.D. Hong, S.B. Kim, K.W. Chung, B.O. Choi, Recessive optic atrophy, sensorimotor neuropathy and cataract associated with novel compound heterozygous mutations in OPA1, Mol. Med. Rep. 14 (2016) 33–40. <https://doi.org/10.3892/mmr.2016.5209>.
- [20] A. Hubstenberger, N. Merle, R. Charton, G. Brandolin, D. Rousseau, Topological analysis of ATAD3A insertion in purified human mitochondria, J. Bioenerg. Biomembr. 42 (2010) 143–150. <https://doi.org/10.1007/s10863-010-9269-8>.

Acknowledgments

The authors would like to acknowledge Association des Maladies Mitochondriales (AMMi), France, for the financial support. . T.W. was supported by the European Research Council (ERC) Starting Grant No. 714472 (Acronym “Mitomorphosis”).

Key words:

Mitochondrial disease

ATAD3A

Sensitive motor neuropathy

Congenital cataract